An angle-based partition design method for offshore wind farm collector systems

Xingru Ye[1], Ronghua Zhu[1], Chenghong Gu[2], Haining Xing[3], Yiwei Hu[2], and Cailiang Zhang[3]

[1]Zhejiang University Ocean College
[2]University of Bath
[3]Advanced Energy Science and Technology Guangdong Laboratory

January 11, 2025

Abstract

This study proposes a novel angle-based partition design method to optimize the collector system of offshore wind farms. It highlights the importance of improving the reliability of the collector system while reducing overall costs. By integrating the minimum spanning tree algorithm with angle-based partition theory, this method minimizes subsea cable lengths and reduces failure risks under constraints such as the number of feeders, subsea cable current capacity, balanced feeder power, and avoidance of cable crossings, thereby enhancing system efficiency and reliability. A case study on a recent 1-GW offshore wind farm in Guangdong, China, was used to validate the effectiveness of the proposed method. A multi-criteria decision analysis approach was used to evaluate the proposed method. The evaluation results showed that the design scheme generated by the angle-based partition method performed the best. This design scheme demonstrated a more balanced distribution of turbines per feeder, with virtually no increase in subsea cable length compared to traditional methods such as Improved Prim and Angle-based K-means Clustering.

Highlights

An angle-based partition design method for offshore wind farm collector systems

Xingru Ye,Ronghua Zhu,Chenghong Gu,Haining Xing,Yiwei Hu,Cailiang Zhang

- Proposes the angle-based partition theory for offshore wind power collector systems to reduce cable failure risks.
- Achieves reduced cable lengths and a balanced distribution of turbines per feeder in the case study, enhancing system stability and cost-effectiveness.
- Simplifies the complexity of traditional approaches and improves scalability through a structured partition framework, making it suitable for multi-phase and multi-zone offshore wind farm projects.
- The application of multi-criteria decision analysis confirms the superior performance of the proposed design across multiple evaluation criteria, highlighting its reliability and efficiency.

An angle-based partition design method for offshore wind farm collector systems

Xingru Ye[a,b,c], Ronghua Zhu[a,d,*], Chenghong Gu[c], Haining Xing[d], Yiwei Hu[c] and Cailiang Zhang[d,e]

[a] *Ocean College, Zhejiang University, Zhoushan, 316000, China*
[b] *Interdisciplinary Student Training Platform for Marine areas, Zhejiang University, Hangzhou, 310027, China*
[c] *Department of Electronic and Electrical Engineering, University of Bath, Bath, BA2 7AY, UK*
[d] *Yangjiang Offshore Wind Energy Laboratory, Yangjiang, 529500, China*
[e] *School of Software & Internet of Things Engineering, Jiangxi University of Finance and Economics, Nanchang, 330013, China*

ARTICLE INFO

Keywords:
Offshore wind
Collector system
Cable failure
Minimum spanning tree
PROMETHEE

ABSTRACT

This study proposes a novel angle-based partition design method to optimize the collector system of offshore wind farms. It highlights the importance of improving the reliability of the collector system while reducing overall costs. By integrating the minimum spanning tree algorithm with angle-based partition theory, this method minimizes subsea cable lengths and reduces failure risks under constraints such as the number of feeders, subsea cable current capacity, balanced feeder power, and avoidance of cable crossings, thereby enhancing system efficiency and reliability. A case study on a recent 1-GW offshore wind farm in Guangdong, China, was used to validate the effectiveness of the proposed method. A multi-criteria decision analysis approach was used to evaluate the proposed method. The evaluation results showed that the design scheme generated by the angle-based partition method performed the best. This design scheme demonstrated a more balanced distribution of turbines per feeder, with virtually no increase in subsea cable length compared to traditional methods such as Improved Prim and Angle-based K-means Clustering.

Nomenclature and acronyms definition

ABKMC	Angle-based K-means Clustering
ABPT	Angle-based Partition Theory
AC	Alternating Current
CCW	Counter-Clockwise
HV	High Voltage
HVAC	High Voltage Alternating Current
HVDC	High Voltage Direct Current
LV	Low Voltage
MST	Minimum Spanning Tree
MV	Medium Voltage
SOP	Soft Open Points
i	Index for feeder
j	Index for turbine
N_s	Node count in a sector
$e_{i,j}$	Cable segment connecting the j-th wind turbine on the i-th feeder
F	Objective function
f	Number of feeders
$f_{\max}$	Maximum number of feeders
$f_{\min}$	Minimum number of feeders
L	Total length of the collector system

*Corresponding author
zhu.richard@zju.edu.cn (R. Zhu)

N	Number of wind turbines connected to each feeder in a regular wind farm
N_i	Number of turbines on the i-th feeder
P_0	Rated power per turbine
$P_{\max}$	Maximum active power allowed for the cable
P_b	Allowable deviation in power transmission between any two feeders
P_i	Power transmitted through the i-th feeder

1. Introduction

1.1. Offshore wind power system

To use the electricity generated by the wind turbines in an offshore wind farm, the electrical system employs subsea cables to interconnect the turbines and transmit power to the grid. Structurally, this system can be divided into three main components: the collector system, the offshore substation, and the transmission system. As shown in Fig. 1, the

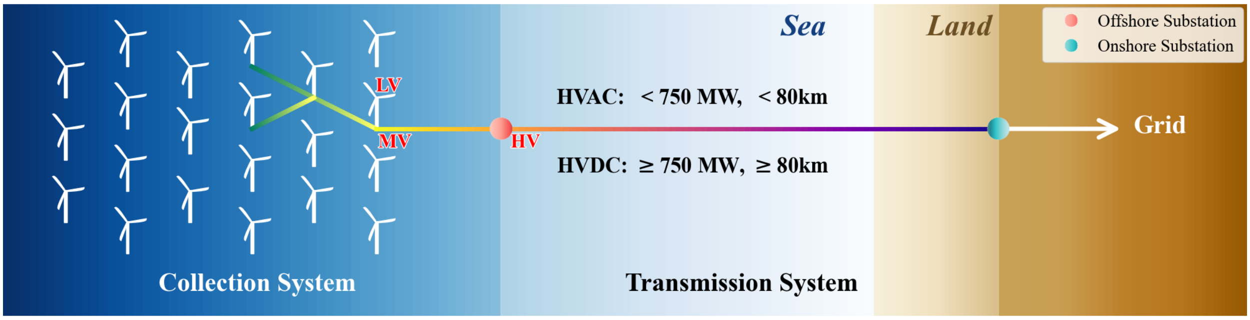

Fig. 1. General representation of offshore wind power system.

collector system typically starts with a transformer located at the base of each wind turbine tower, which steps up the voltage from Low Voltage (LV) to Medium Voltage (MV). The collector system always uses AC inter-array subsea cables to collect energy from wind turbines. Then, an array of MV subsea cables connects the output from wind turbines to the offshore substation. The offshore substation aggregates power from multiple feeders arranged in a specified main wiring configuration and steps up the voltage as required. Finally, the transmission system employs High Voltage (HV) subsea cables to integrate the offshore wind farm with the onshore substation [1, 2].

Inter-array and export cables are critical components of offshore wind farms. Specifically, inter-array cables transmit electricity from turbines to offshore substations, while export cables carry the collected power from offshore substations to onshore substations. A study conducted by the University of Strathclyde [3] found that the average rate of cable failure in European offshore wind farms is approximately 0.003 failures/km/year. This statistic translates to a 30% chance of cable failure for an offshore wind farm with 100 km of cables in any given year. The consequences of such failures can be significant; the average downtime for repairing inter-array cables is around 40 days, while export cable repairs take about 60 days. This prolonged repair time exacerbates energy losses and incurs substantial economic costs. To address these challenges, reducing cable lengths can be beneficial as it reduces operation and maintenance expenses by reducing failure risks. However, the layout of turbines and the placement of substations are influenced by multiple factors, including offshore wind resources, terrain, and navigation-restricted areas [4], all of which limit the extent to which the total length of export cables can be minimized. In contrast, there remains significant potential for optimizing the layout of inter-array cables within the collector system, allowing for reductions in overall cable length and enabling substantial cost savings.

There are generally two typical topologies for collector systems: radial and ring [5], as shown in Fig. 2a and Fig. 2b. Some literature also mentions star topology [6, 7] as shown in Fig. 2c, characterized by each generator having its dedicated feeder. However, independent commercial applications of star topology are rare; it is often combined with radial topology to form tree variant, as shown in Fig. 2d. Another hybrid variant, mesh, combines the topologies above, shown in Fig. 2e. The characteristics, advantages, disadvantages, and typical cases of the four common grid topologies are summarized in Table 1, among which the offshore wind farm figures are from the KIS-ORCA Project [8].

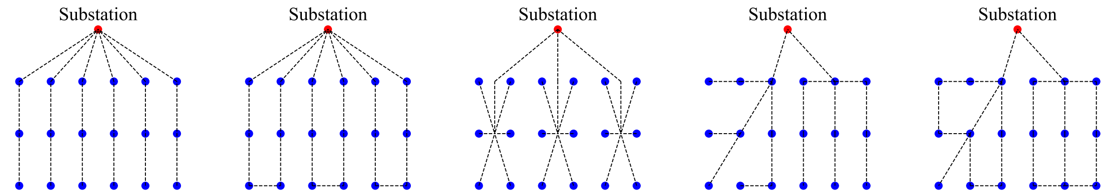

(a) Radial. **(b)** Ring. **(c)** Star. **(d)** Tree. **(e)** Mesh.

Fig. 2. Collector system topologies.

Notably, in a general ring topology, all cables need to be designed for a maximum current to ensure power transmission to the substation in the event of a cable fault. Another special ring topology only uses a cable with the smallest cross-section to tie feeder-terminal turbines. The adjacent feeder provides basic power through the tie cable after a feeder failure to ensure continuous operation of critical turbine systems such as heating, dehumidification, control, and yaw, thereby maintaining turbine safety. These two ring types are not commonly used in offshore wind farms due to high investment costs and low economic feasibility. In recent years, most commercial offshore wind farms, whether fully commissioned, under construction, or consent-authorized, have adopted either a radial or tree topology.

1.2. Optimization of collector systems

Most optimization problems of the collector system aim to minimize the total cable length [9]. Several feasible strategies for optimizing collector systems have been proposed based on various demands and constraints like restricted areas, power generation, cable networks, and energy loss. For instance, Dutta and Overbye present three new algorithms for designing wind farm cable layouts: improving the Minimum Spanning Tree (MST), limiting turbine connections per feeder, and optimizing cable sizes based on power flow [10]. However, introducing Steiner points can make branches more vulnerable [11]. Huang et al. optimize and solve the problem on its sub-regional levels using the combination of graph theory and the improved fuzzy C-means algorithm [12]. Hou et al. optimize the location of offshore substation and the collector system layout by Prim algorithm [13]. Later, they use the fuzzy C-means algorithm to partition the wind farm and optimize the location of offshore substations in each sub-region instead of relying on clustering centers and apply the adaptive PSO-MST algorithm to create uncrossed cable connection layouts for both the collector system and transmission system [14, 15]. Also, some research introduces the obstacle constraint and uses mixed integer linear programming to solve the optimization problem [16, 17]. Wu et al. present a hybrid optimization approach combining meta-heuristic algorithms and geographic information systems to simultaneously optimize the site selection, three-dimensional wind turbine layout, and cable routing for offshore wind farms [4]. Song proposes a bi-level constrained optimization model based on maximum profit and the shortest route of cable and uses a differential evolution and improved Prim algorithm to optimize the model [18]. Zuo et al. design a hybrid GA-ST-MST optimization approach in wind farm cable system optimization [19].

However, previous studies focus on certain extreme constraints, without considering the balance of feeder power capacity or the standardization of subsea cable installation and maintenance. In addition, the optimization of the collector system relies on clustering algorithms and metaheuristic algorithms, making the established models overly complex. Some multi-layer models and synchronized optimization designs lack practical feasibility in engineering applications. This leads to poor scalability of the collector system, especially in the context of multi-phase and multi-zone construction of offshore wind farms.

1.3. Contributions

To address the issue above, the Angle-based Partition Theory (ABPT) is proposed to optimize cable layouts in collector systems. Although primarily developed for offshore wind farm grids, this method is also applicable to other scenarios, such as exhaustive foraging for stationary targets, demonstrating its contribution to advancements in graph theory algorithms.

Table 1
Comparison of collector system topologies.

Topology	Typical	
	Radial	**Ring**
Characteristic	Several generators are connected along a single feeder that travels to the substation, along with other feeders.	Similar to the radial grid but with the back ends of the feeders connected together.
Advantage	**Simple and cheap:** The system structure is the simplest, the total length of cables is small, and the cost can be effectively reduced by reducing the diameter of the subsea cable.	**More reliable:** If one path fails, another path can be used.
Disadvantage	**Lack of reliability:** If one feeder fails, all generators connected to that feeder will not produce power.	**More costly:** To account for any cable failure, the current flow is not constant; all cables must handle maximum current, requiring a larger cross-section and higher investment.
Case	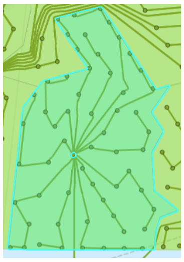 Hornsea 1 (West), UK, 2019	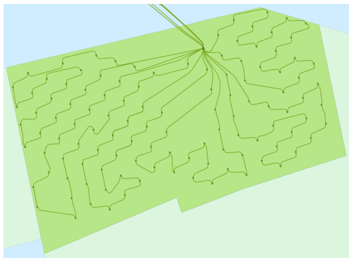 Rampion, UK, 2018

Topology	Variant	
	Tree	**Mesh**
Characteristic	Similar to the radial grid, but allows branches.	A combination of the previous three topologies.
Advantage	Similar to the radial grid, however, it is more flexible and can further reduce the cable length, thereby lowering the cost.	The system has higher reliability and redundancy.
Disadvantage	Lack of reliability and more complex in route planning.	The grid structure is complex, and the cost is high.
Case	 Westermost Rough, UK, 2022	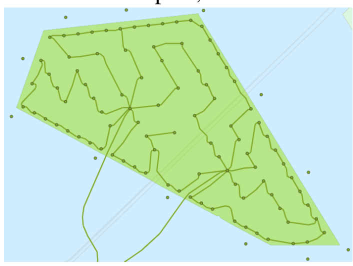 Triton Knoll, UK, 2022

The rest of this paper is organized as follows. Section 2 details the optimization process for collector systems using ABPT. Section 3 presents case studies to illustrate the application of ABPT, and Section 4 concludes the paper.

2. Collector system optimization

2.1. Optimization objective

As we mentioned in Section 1, minimizing the total length of the collector system can help reduce cable failure risks, so the optimization aims to minimize the total length. The objective function can be represented as:

$$F = \min L = \min \sum_{i=1}^{f} l_i = \min \sum_{i=1}^{f} \sum_{j=1}^{N_i} \left| e_{i,j} \right| \quad (1)$$

$$\mathbf{E} = \{ e_{i,j} \mid i \in 1, 2, \ldots, f, \; j \in 1, 2, \ldots, N_i \} \quad (2)$$

In the equation, L is the total length of the collector system; f is the number of feeders; N_i is the number of turbines on the i-th feeder. The set $\mathbf{E}$ represents all cable segments in the system, where each element $e_{i,j}$ represents the cable segment connecting the j-th wind turbine on the i-th feeder.

The lengths of the cables are calculated according to the geometrical distance without considering practical usage, such as barriers or restrictions in the sea. The condition of two or more cables failing in one feeder can be neglected since the probability is minuscule.

2.2. Optimization constraints

2.2.1. Feeder amount constraints

In a collector system, the number of cable entries at the substation is limited by the number of input terminals on the transformer. Too many cable entries can affect the topology's economic efficiency. At the same time, too few entries can result in excessive power transmission through the incoming subsea cables, compromising the safe operation of the entire topology. Therefore, the number of feeders connected to the substation must lie within the permissible range:

$$f_{\min} \leqslant f \leqslant f_{\max} \tag{3}$$

where $f_{\min}$ and $f_{\max}$ are the minimum and maximum numbers of feeders to the substation, respectively.

2.2.2. Cable carrying capacity constraints

Due to the limited carrying capacity of subsea cables, each feeder should not connect too many wind turbines to exceed the carrying capacity. Since the turbine models and voltage levels in the same wind farm are usually consistent, the constraint on the maximum number of turbines per feeder can be expressed as:

$$N_i \leqslant \lfloor \frac{P_{\max}}{P_0} \rfloor \quad \forall i \in \{1, 2, \dots, f\} \tag{4}$$

where $P_{\max}$ is the maximum active power allowed for the cable; P_0 is the rated power per turbine.

2.2.3. Balancing power

Ensuring similar power input from each feeder to the substation offers several benefits, particularly in facilitating the economic selection of subsea cables. The procurement of cables can be optimized to ensure uniform specifications, simplifying the selection process and reducing costs. Additionally, this standardization improves resource allocation and load distribution, enhancing system stability by preventing over-load or under-load conditions. Thereby, it reduces power losses, improves transmission efficiency, and simplifies maintenance. Finally, evenly distributed power extends the lifespan of equipment by avoiding overloading specific components. Overall, balancing power input improves operational efficiency and reliability and facilitates cost-effective cable selection. To ensure power balance among feeders:

$$\left| P_i - P_j \right| \le \Delta P_{\mathrm{b}} \quad \forall i, j \in \{1, 2, \dots, f\} \tag{5}$$

where P_i is the power transmitted through the i-th feeder and ΔP_{b} is the allowable deviation in power transmission between any two feeders. Equation 5 can be written in another way:

$$\left| N_i - N_j \right| \le \lfloor \frac{\Delta P_{\mathrm{b}}}{P_0} \rfloor \quad \forall i, j \in \{1, 2, \dots, f\} \tag{6}$$

2.2.4. Cross-avoidance constraints

The crossing of cables in the subsea environment poses significant challenges for construction and can also impact the safe operation of the collector system. Therefore, the collector system should avoid subsea cable crossings.

$$e_{i_1,j_1} \cap e_{i_2,j_2} = \emptyset \quad \forall e_{i_1,j_1}, e_{i_2,j_2} \in \mathbf{E}, \quad (i_1, j_1) \neq (i_2, j_2) \tag{7}$$

2.3. Flowchart of proposed method

The optimization problem is simplified into a shortest-path design problem. It is realized by efficiently distributing tasks and minimizing resource consumption. Fig. 3 illustrates the flow of the proposed method, consisting of several key stages:

1. Divide nodes into sectors based on angles.
2. Distribute unassigned nodes to nearby sectors.
3. Use MST algorithm.
4. Calculate the total path length.

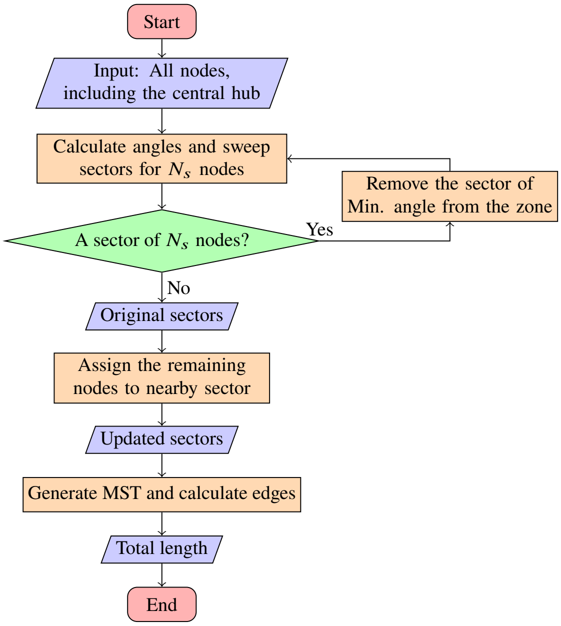

Fig. 3. Flowchart of ABPT.

2.4. Divide nodes into sectors based on angles

The initial phase of the method focuses on dividing nodes into sectors according to their angles relative to the central hub, as shown in Fig. 4. To begin, assign an initial node count N_s to each sector based on the limits of the final path. Then, using the central hub as the centre of the sweep, sweep the entire zone to identify sectors that can cover N_s nodes while minimizing the angle. Once a sector is found, sweep the remaining zone for the next sector that can also cover N_s nodes with the smallest angle. Continue this process iteratively until no additional sectors meeting the criteria can be found. Fig. 4c shows the first three sectors swept in a counterclockwise direction. To help readers understand better, we take $N_s = 5$ as an example. At this stage, the initial segment of sectors and assignment of nodes is complete. Most nodes will have been distributed to their respective sectors, while a few may remain unassigned. As shown in Fig. 4d, S_1 and S_2 are the two sectors with the smallest angles that can cover N_s nodes, and two nodes remain unassigned.

2.5. Distribute unassigned nodes to nearby sectors

Angular differences between each unassigned node and assigned nodes relative to the central hub are calculated. Each unassigned node is then assigned to the sector that corresponds to the assigned node with the smallest angular difference. As a result of the assignment, the sectors S_1 and S_2 update into S_1' and S_2'. The new partition is shown in Fig. 5a.

2.6. Use MST algorithm

In this stage, generating an MST for each sector helps determine the shortest paths that connect nodes to the central hub, as shown in Fig. 5b. MST is a concept from graph theory and is commonly used to solve problems related to network design, optimization, and minimizing connection costs [20]. It aims to find a subset of edges in a weighted graph that connects all vertices together without forming any cycles while minimizing the total edge weight. This loopless edge selection feature, combined with the minimization of total edge weight, ensures no crossings in the MST. Kruskal and Prim are two common algorithms for finding the MST. Kruskal algorithm selects the smallest weight edge at each step and adds it to the tree until all vertices are connected, making it well-suited for sparse graphs. Prim algorithm, on the other hand, starts from a specific vertex and expands the tree by adding the minimum weight edge that connects a vertex inside the tree to one outside, making it more efficient for dense graphs. For each sector's

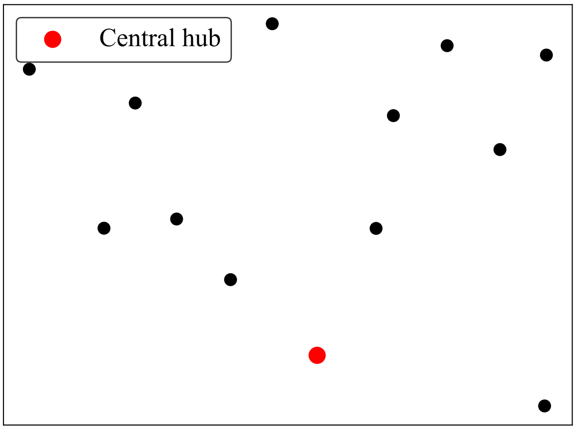

(a) Nodes layout.

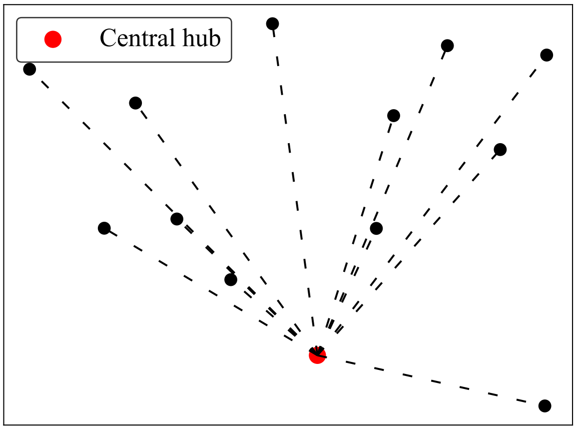

(b) Calculate the angle.

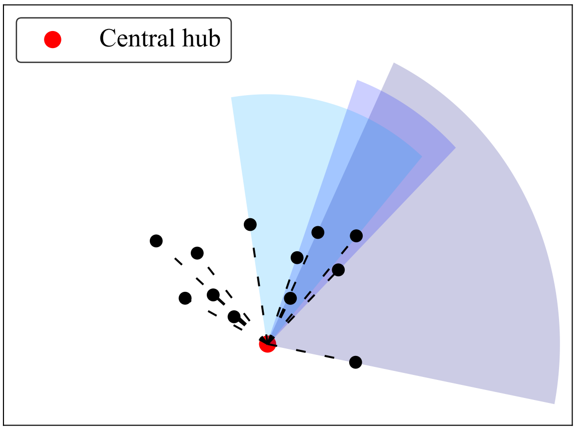

(c) Sector sweeping.

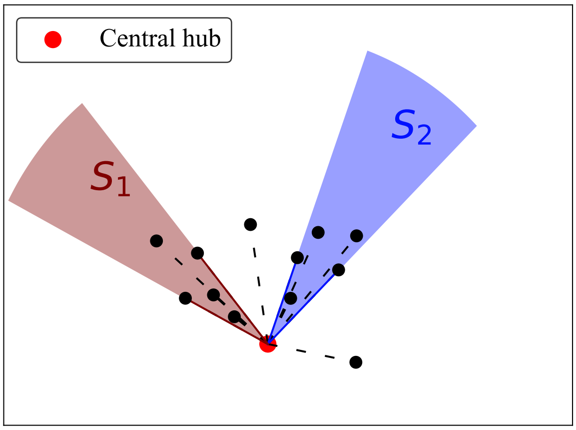

(d) Sectors of N_s nodes.

Fig. 4. Divide nodes into sectors based on angles.

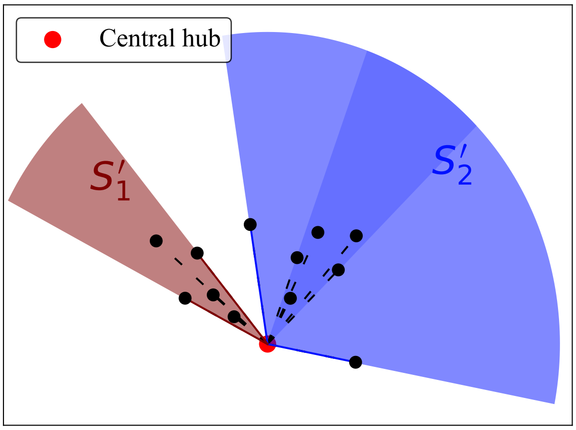

(a) Update sectors.

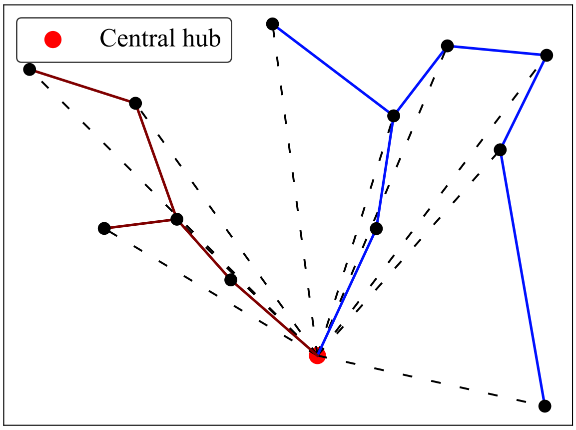

(b) MST for sectors.

Fig. 5. Distribute unassigned nodes and generate MST.

MST generation, the central hub should be added to the sector first to guarantee the sector nodes are connected from the central hub. Utilizing MST's acyclic and non-intersecting characteristics, we ensure that paths within each sector do not cross. Additionally, by previously ensuring the sectors themselves do not overlap during the partitioning process, the entire generated path remains free of intersections.

2.7. Calculate the total path length

Finally, the total path length of the entire system is calculated. This involves summing the lengths of the edges generated by the MSTs across all sectors. By minimizing the total path length, the method ensures that the distance from the central hub to all other nodes is optimized under the initial N_s, thus reducing resource usage.

3. Case study

3.1. Dataset

This paper selects a two-zone offshore wind farm project in Guangdong, China. Zone 1 has an approximate total installed capacity of 400 MW, with 37 units of 11-MW turbines numbered 1 to 37. Zone 2 has an approximate total installed capacity of 600 MW, with 55 units of 11-MW wind turbines numbered 38 to 92. The offshore wind farm is equipped with a 500 kV offshore substation, 16 feeders of 66 kV array cables, and 2 feeders of 500 kV export subsea cables. The original collector system of the offshore wind farm is shown in Fig. 6, and the connection details for each feeder are provided in Table 2. This wind farm is arranged in a radial layout, with a total feeder length of 141,958.00 meters for the collector system.

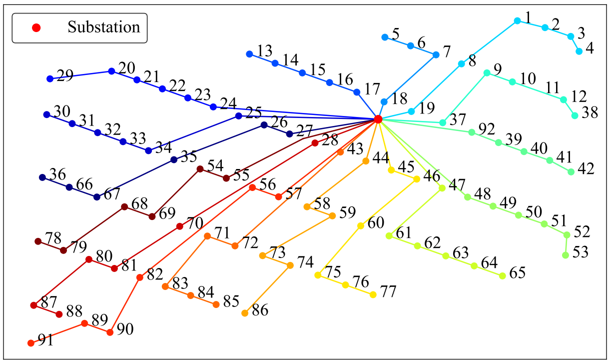

Note: Lines of the same color belong to the same feeder. Colors are used for clarity and do not indicate functional differences.

Fig. 6. The original collector system of the offshore wind farm.

3.2. Parameter setting

Parameters are set based on the constraints in Section 2.2. For cable carrying capacity, a single-core 1600 mm^2 cross-linked polyethylene cable with a rated voltage of 66 kV can theoretically transmit a maximum power of 174 MW [21]. According to Equation (4), $N \leqslant \lfloor 174\,\mathrm{MW}/11\,\mathrm{MW} \rfloor = 15$ turbines. The minimum limitation of incoming cables of the substation $f_{\min} = \lceil 92/15 \rceil = 7$. The maximum limitation of incoming cables of the substation can be assumed at the original feeder amount, i.e., $f_{\max} = 16$.

In Section 2.4, the initial number of nodes assigned to each sector is N_s. If the nodes are unevenly distributed around the central hub, the final number of nodes assigned to each sector should fall within the range $[N_s, N_s+2(N_s-1)]$, i.e., $[N_s, 3N_s-2]$. However, in practice, the layout of offshore wind farms tends to be more regular, so it can be assumed that after reallocation, the number of wind turbines connected to each feeder, denoted as N, most likely will be within the range $[N_s, N_s+2(N_s-1)/2]$, i.e., $[N_s, 2N_s-1]$. It is appropriate to set the initial value of N_s to an integer between 4 and 8.

3.3. Benchmarks

This paper uses two methods, Improved Prim and Angle-based K-means Clustering (ABKMC), as benchmarks for comparison. Both methods share certain similarities with our proposed methods.

Table 2
Feeders of the collector system.

Line No.	Connection sequence from the substation
1	27 → 26 → 35 → 67 → 66 → 36
2	25 → 34 → 33 → 32 → 31 → 30
3	24 → 23 → 22 → 21 → 20 → 29
4	17 → 16 → 15 → 14 → 13
5	18 → 7 → 6 → 5
6	19 → 8 → 1 → 2 → 3 → 4
7	37 → 9 → 10 → 12 → 38
8	92 → 39 → 40 → 41 → 42
9	48 → 49 → 50 → 51 → 52 → 53
10	47 → 61 → 62 → 63 → 64 → 65
11	45 → 46 → 60 → 75 → 76 → 77
12	44 → 58 → 59 → 73 → 74 → 86
13	43 → 72 → 71 → 83 → 84 → 85
14	57 → 56 → 82 → 90 → 89 → 91
15	28 → 70 → 81 → 80 → 87 → 88
16	55 → 54 → 69 → 68 → 79 → 78

3.3.1. Improved Prim

Improved Prim is an enhancement of Prim that incorporates the constraints on the number of feeders. The specific steps of Improved Prim are as follows.

Distance calculation and sorting Calculate the distances from all turbine nodes to the substation and sort the nodes in ascending order based on their distances.

Connection of closest nodes According to the number of feeders f, connect f nodes closest to the substation and mark them as visited, adding these connections into the array `Edges`.

Edge selection For each unmarked node, select the edge with the minimum weight connecting them to the marked nodes. Check whether this edge intersects with any edge in the array `Edges`. The Counter-Clockwise (CCW) orientation test [22, 11] is often used to check whether two edges intersect:

1. Check Shared Endpoints: Assume A and B are endpoints of edge E_1, and C and D are endpoints of edge E_2. If any endpoints are identical between E_1 and E_2 (e.g., $A = C$), then we define the edges as not intersecting in a strict geometric sense, as they merely share a point without truly crossing.
2. Check Relative Orientation: Calculate the CCW values for (A, B, C) and (A, B, D) :

   $$\mathrm{CCW}(A, B, C) = (C_y - A_y)(B_x - A_x) - (B_y - A_y)(C_x - A_x) \tag{8}$$

   If $\mathrm{CCW}(A, B, C) > 0$, the points are in a counterclockwise orientation. If $\mathrm{CCW}(A, B, C) < 0$, the points are in a clockwise orientation.

   If the orientations of (A, B, C) and (A, B, D) differ, C and D lie on opposite sides of edge E_1.

   Similarly, the CCW values for (A, C, D) and (B, C, D) are computed. If these orientations differ, A and B lie on opposite sides of edge E_2.
3. Determine Intersection: The two edges intersect only if the orientations of (A, B, C) and (A, B, D) differ and the orientations of (A, C, D) and (B, C, D) differ.

If they do not intersect, mark the turbine node as visited and add the edge to the array `Edges`; if they intersect, discard this edge and select the next smallest edge, repeating the intersection check.

Optimization completion Once all nodes are marked, the optimization of the collector system is complete.

Table 3
Characteristics of the collector system for different initial node count using the ABPT method.

Initial No. of nodes N_s	**4**	**5** ①	**6** ②	**7** ③	**8** ④
No. of feeders f	17	13	12	11	10
Total length (m)	149975	130403	124873	117037	116029
Min. length of feeders (m)	4232	6938	7167	7167	7664
Max. length of feeders (m)	13587	16541	16541	15922	16541
Min. turbine count per feeder	4	5	6	7	8
Max. turbine count per feeder	7	12	12	12	12
Meet the limit?	No	Yes	Yes	Yes	Yes

3.3.2. ABKMC

The ABKMC method we propose is inspired by Angle-based clustering [23], but it differs fundamentally in its approach. This method clusters wind turbine nodes based on their angular relationships to the substation. The specific steps of ABKMC are as follows.

Angle calculation Calculate the angle of each turbine node relative to the substation.

K-means clustering Perform K-means clustering on the angle values. To enhance the stability and reliability of K-means clustering on angle values, multiple runs are performed to build a consensus matrix, accounting for variations in the initial clustering centers. The number of clusters is set to match the number of feeders f.

Hierarchical clustering Apply a hierarchical clustering algorithm to the consensus matrix to obtain the final cluster labels.

MST generation Finally, augment each cluster with the substation to generate their respective MST.

3.4. Results and analysis

Using the ABPT method proposed in this paper, setting the initial number of sector nodes N_s from 4 to 8, the automatic optimization results of the collector system are shown in Fig. 7. The first subfigure in each row represents the initial sector partition under N_s, where the turbine nodes connected to the substation by solid lines of the same colour indicate that they are assigned to the same sector, while the remaining blue points connected to the substation by dashed lines represent unassigned points. The second subfigure shows the result of updated sectors. The third subfigure illustrates the result of generating an MST for each sector, where the feeder connects all the nodes within the sector. It's hard to tell the difference of the final scheme directly from the figure, so we compare the characteristics in Table 3. When N_s is set between 5 and 8, the feeder constraints are satisfied. Increasing N_s typically leads to a reduction in the number of feeders and total length. This is because during the partition process, the more nodes assigned to each sector, the fewer sectors there are to divide, leading to fewer limitations on the entire system, which approaches the process of creating an MST for the entire system. When N_s is set to 8, the difference between the maximum and minimum number of turbines connected to a single feeder is the smallest, which best meets the power balance requirements. There are no significant differences in other characteristics when N_s varies from 5 to 8.

Fig. 8 shows the results of two benchmarks. From Fig. 8a, we can see that the Improved Prim method has significant weaknesses. It leads to a very uneven distribution of wind turbines on the feeders. Particularly in cases where there are too many turbines on a single feeder, it exceeds the cable's power transmission limits. As shown in Fig. 8b, the ABKZ method results in a more balanced distribution of wind turbines across the feeders compared to the Improved Prim. However, it's hard to distinguish its differences from the ABPT method, so the characteristics are also listed in Table 4. It shows that when the number of feeders f is set between 11 and 16, the maximum limit of turbines connected to a single feeder is satisfied. However, the number of turbines connected to each feeder is uneven, with differences reaching up to 3 to 4 times.

Since the design scheme ①-⑩ all meet the design constraints, and the difference in total length is not particularly significant, this research uses a multi-criteria decision analysis (MCDA) method to rank the design schemes from best to worst. The weights of the criteria are found by the analytic hierarchy process (AHP) and then the Preference Ranking

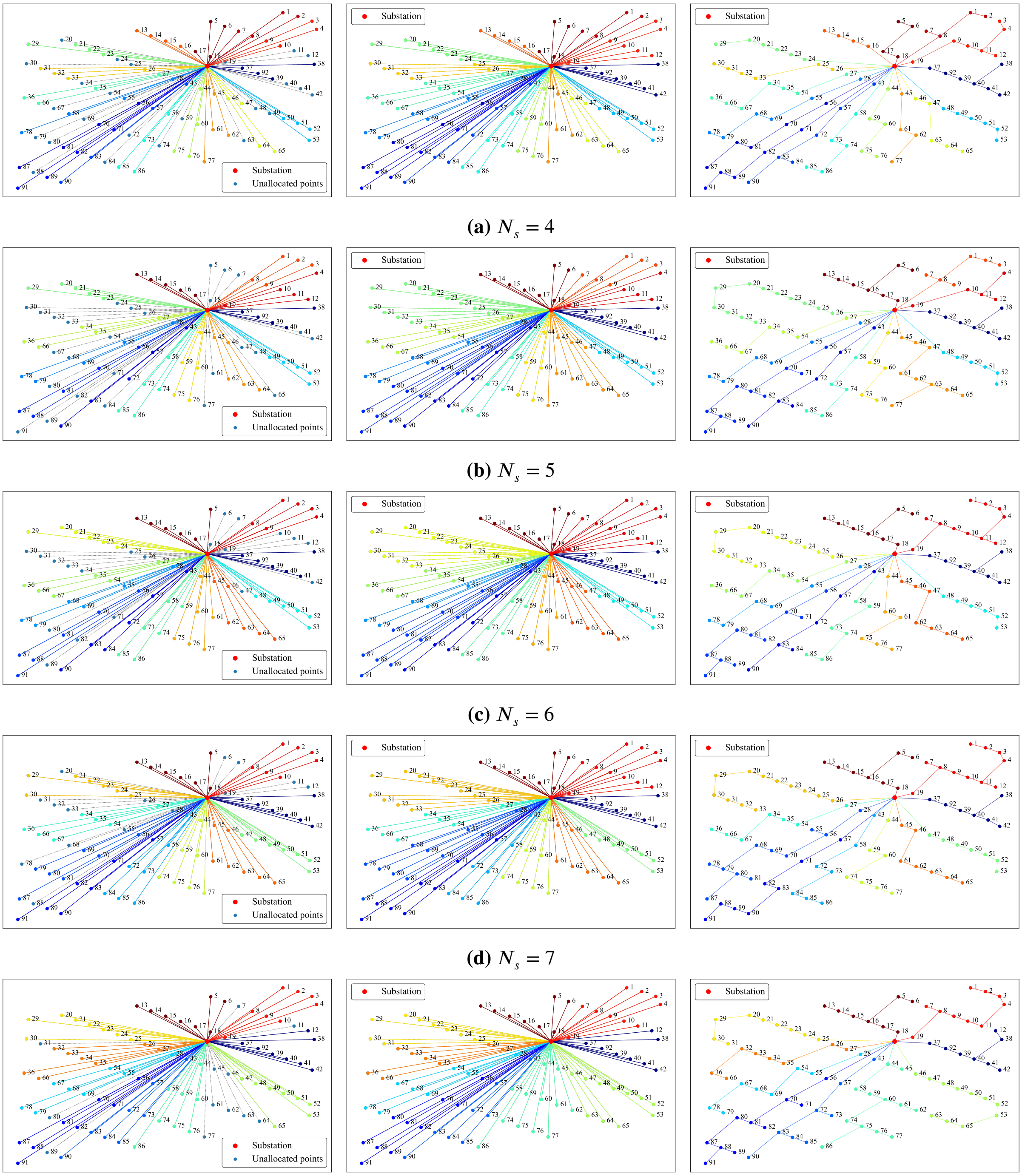

(a) $N_s = 4$

(b) $N_s = 5$

(c) $N_s = 6$

(d) $N_s = 7$

(e) $N_s = 8$

Fig. 7. Automatic optimization process using the ABPT method.

Organization Method for Enrichment of Evaluations (PROMETHEE) II is applied by using those weights to select the best scheme [24].

The evaluation is based on six criteria: 1. Number of feeders, 2. Total length, 3. Maximum difference of feeder lengths, 4. Maximum difference of turbine count on feeders, 5. Standard deviation (SD) of feeder lengths, and 6. SD of

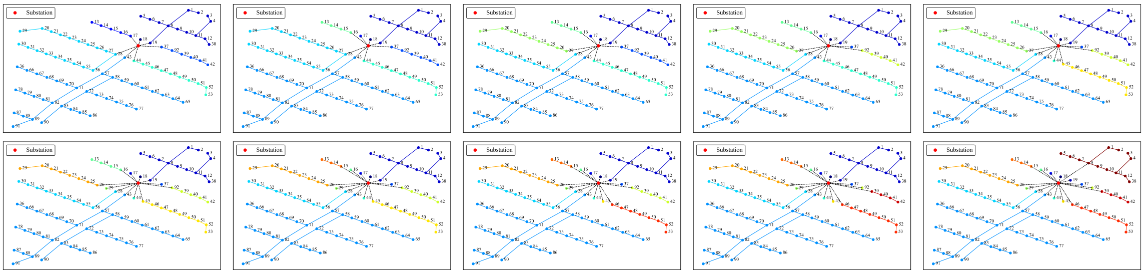

(a) Improved Prim (f from 7 to 16).

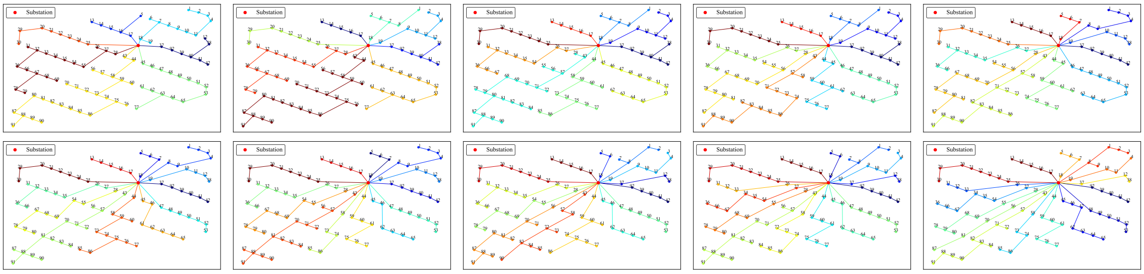

(b) ABKZ (f from 7 to 16).

Fig. 8. Results of benchmarks.

Table 4
Characteristics of the collector system for different feeder counts using the ABKZ method.

No. of feeders f	**7**	**8**	**9**	**10**	**11 ⑤**
Total length (m)	97821	99503	102711	109644	109749
Min. length of feeders (m)	6721	4312	4312	4312	4312
Max. length of feeders (m)	27646	27646	24519	20282	19540
Min. turbines per feeder	6	5	5	5	4
Max. turbines per feeder	26	26	22	16	15
Meet the limit?	No	No	No	No	Yes
No. of feeders f	**12 ⑥**	**13 ⑦**	**14 ⑧**	**15 ⑨**	**16 ⑩**
Total length (m)	112868	118618	126929	128086	137031
Min. length of feeders (m)	4312	4312	4109	4109	4312
Max. length of feeders (m)	19420	19420	16541	17938	16509
Min. turbines per feeder	4	4	3	3	3
Max. turbines per feeder	15	15	10	12	11
Meet the limit?	Yes	Yes	Yes	Yes	Yes

turbine count on feeders. Table 5 presents the pairwise comparison matrix used in the AHP to determine the weights of the six evaluation criteria. Each element in the matrix represents the relative importance of one criterion compared to another, using Saaty's 9-point scale. For example, the importance of "total length" compared to "number of feeders" is rated as 7, indicating that "total length" is considered much more significant. After processing the matrix through AHP calculations, the normalized weights for each criterion are derived as follows: 0.080, 0.463, 0.031, 0.039, 0.134, and 0.253. The criterion "total length" (0.463) and "SD of turbine count on feeders" (0.253) have the most significant impact on the rankings, while "Max Diff. of feeder length" (0.031) and "Max Diff. of turbine count" (0.039) have less influence.

The evaluation results are presented in Table 6. All the values have been normalized and each design scheme is ranked according to the weighted sum of the criteria. Except for the criterion "No. of feeders", which is better when

Table 5
Pair-wise comparison matrix.

Criterion	No. of feeders	Total length	Max Diff. of feeder lengths	Max Diff. of turbine count	SD of feeder lengths	SD of turbine count on feeders
No. of feeders	1	1/7	3	3	1/3	1/5
Total length	7	1	9	7	5	3
Max Diff. of feeder lengths	1/3	1/9	1	1/3	1/5	1/7
Max Diff. of turbine count	1/3	1/7	3	1	1/3	1/5
SD of feeder lengths	3	1/5	5	3	1	1/3
SD of turbine count on feeders	5	1/3	7	5	3	1

Table 6
Preference ranking of alternatives.

Criterion	Original	①	②	③	④	⑤	⑥	⑦	⑧	⑨	⑩	Weight
No. of feeders	1.00	0.50	0.33	0.17	0.00	0.17	0.33	0.33	0.67	0.83	1.00	
1-No. of feeders	0.00	0.50	0.67	0.83	1.00	0.83	0.67	0.67	0.33	0.17	0.00	0.08
Total length	1.00	0.64	0.47	0.23	0.19	0.00	0.10	0.28	0.53	0.57	0.85	0.46
Max Diff. of feeder lengths	0.84	0.43	0.27	0.05	0.00	0.18	0.27	0.45	0.70	0.74	1.00	0.03
Max Diff. of turbine count	0.00	0.56	0.44	0.33	0.22	1.00	1.00	1.00	0.56	0.78	0.67	0.04
SD of feeder lengths	0.21	0.06	0.00	0.11	0.12	1.00	0.78	0.62	0.57	0.42	0.27	0.13
SD of turbine count on feeders	0.00	0.52	0.52	0.45	0.29	1.00	0.82	0.76	0.59	0.59	0.48	0.25
Total	0.52	0.51	0.43	0.32	0.27	0.50	0.46	0.51	0.54	0.54	0.61	
Preference ranking	8	7	3	2	1	5	4	6	10	9	11	

larger, all other criteria are harmful. Therefore, the values of "No. of feeders" are inverted, and the alternative with the smallest final score is considered the optimal solution.

The design scheme ④ ranks the highest with the smallest score of 0.27, indicating it performs best across the selected criteria. On the other hand, the design scheme ⑩, with a score of 0.61, ranks the lowest, showing it is the least optimal.

4. Conclusion

In conclusion, the proposed angle-based partition method, integrated with the MST algorithm, effectively optimizes the collector system for offshore wind farms by minimizing subsea cable lengths while ensuring a balanced distribution of feeder power. It helps reduce cable failure risks, contributes to the standardized laying of feeders, and reduces subsea cable installation and maintenance costs. The case study conducted on a 1-GW offshore wind farm in Guangdong, China, demonstrated the method's ability to generate a well-balanced design that minimizes cable length while improving system reliability compared to traditional methods like Improved Prim and Angle-based K-means Clustering. The multi-criteria decision analysis further confirmed the superior performance of the proposed approach in terms of turbine distribution per feeder and system efficiency.

Unlike traditional optimization methods that often rely on complex clustering and metaheuristic algorithms, the proposed method offers a simpler and more practical solution. Additionally, the angle-based partition method enhances scalability by providing a structured yet flexible framework, making it well-suited for multi-phase and multi-zone offshore wind farm construction. This ensures that the collector system can adapt effectively to evolving project scales.

However, the method does have limitations. Specifically, it can only generate the optimal design for a given initial node count, which determines the starting partition of the system. While it finds the design with the smallest cable length under the given constraints, it does not guarantee the absolute optimal solution. To obtain the truly optimal design, multiple schemes must be evaluated and compared. Future research could focus on addressing this limitation by exploring methods to dynamically adjust the initial node count.

CRediT authorship contribution statement

Xingru Ye: Conceptualization, Methodology, Software, Formal analysis, Investigation, Validation, Writing – original draft. **Ronghua Zhu:** Supervision, Writing – review & editing. **Chenghong Gu:** Supervision, Writing – review & editing. **Haining Xing:** Writing – review & editing. **Yiwei Hu:** Writing – review & editing. **Cailiang Zhang:** Writing – review & editing.

Declaration of competing interest

The authors declare that they have no known competing financial interests or personal relationships that could have appeared to influence the work reported in this paper.

Acknowledgement

This research is financially supported by the National Natural Science Foundation of China (Grant No. 52371293) and the Key-Area Research and Development Program of Guangdong Province (Grant No. 2021B0707030002).

References

[1] Padmavathi Lakshmanan, Ruijuan Sun, and Jun Liang. Electrical collection systems for offshore wind farms: A review. *CSEE Journal of Power and Energy Systems*, 7(5):1078–1092, 2021.

[2] BVG Associates. Guide to a floating offshore wind farm published on behalf of the offshore renewable energy catapult, the crown estate and crown estate scotland, 5 2023.

[3] John Warnock, David McMillan, James Pilgrim, and Sally Shenton. Failure rates of offshore wind transmission systems. *Energies*, 12(14), 2019.

[4] Yan Wu, Tianqi Xia, Yufei Wang, Haoran Zhang, Xiao Feng, Xuan Song, and Ryosuke Shibasaki. A synchronization methodology for 3d offshore wind farm layout optimization with multi-type wind turbines and obstacle-avoiding cable network. *Renewable Energy*, 185:302–320, 2022.

[5] J.P. Coelingh, A.J.M. van Wijk, and A.A.M. Holtslag. Analysis of wind speed observations on the north sea coast. *Journal of Wind Engineering and Industrial Aerodynamics*, 73(2):125–144, 1998.

[6] Himanshu J. Bahirat, Bruce A. Mork, and Hans Kr. Høidalen. Comparison of wind farm topologies for offshore applications. In *2012 IEEE Power and Energy Society General Meeting*, pages 1–8, 2012.

[7] Max Alexander Parker and Olimpo Anaya-Lara. Cost and losses associated with offshore wind farm collection networks which centralise the turbine power electronic converters. *IET renewable power generation.*, 7(4), 2013-07.

[8] The Kingfisher Information Service - Offshore Renewable & Cable Awareness project (KIS-ORCA). Kis-orca map, 2024.

[9] Xuan Gong, Stefanie Kuenzel, and Bikash C. Pal. Optimal wind farm cabling. *IEEE Transactions on Sustainable Energy*, 9, 2018.

[10] Sudipta Dutta and Thomas J. Overbye. Optimal wind farm collector system topology design considering total trenching length. *IEEE Transactions on Sustainable Energy*, 3(3):339–348, 2012.

[11] Xinwei Shen, Qiuwei Wu, Hongcai Zhang, and Liming Wang. Optimal planning for electrical collector system of offshore wind farm with double-sided ring topology. *IEEE Transactions on Sustainable Energy*, 14(3):1624–1633, 2023.

[12] Huang Ling-ling, Chen Ning, Zhang Hongyue, and Fu Yang. Optimization of large-scale offshore wind farm electrical collection systems based on improved fcm. In *International Conference on Sustainable Power Generation and Supply (SUPERGEN 2012)*, pages 1–6, 2012.

[13] Peng Hou, Weihao Hu, and Zhe Chen. Offshore substation locating in wind farms based on prim algorithm. In *IEEE Power and Energy Society General Meeting*, volume 2015-September, pages 1–5, 2015.

[14] Peng Hou, Weihao Hu, and Zhe Chen. Optimisation for offshore wind farm cable connection layout using adaptive particle swarm optimisation minimum spanning tree method. *IET Renewable Power Generation*, 10, 2016.

[15] Peng Hou, Weihao Hu, Cong Chen, and Zhe Chen. Overall optimization for offshore wind farm electrical system. *Wind Energy*, 20, 2017.

[16] Martina Fischetti and David Pisinger. Optimizing wind farm cable routing considering power losses. *European Journal of Operational Research*, 270, 2018.

[17] Arne Klein and Dag Haugland. Obstacle-aware optimization of offshore wind farm cable layouts. *Annals of Operations Research*, 272, 2019.

[18] Erping Song. A bi-level programming model and differential evolution for optimizing offshore wind farm layout. *Energy Science and Engineering*, 11:2775–2792, 8 2023.

[19] Tengjun Zuo, Yuchen Zhang, Liansong Xiong, Xiangjing Su, Xiaolian Zhang, Ke Meng, Zhao Yang Dong, Haitao Liu, and Sipeng Hao. Complete joint-optimization for offshore wind farm planning. *International Journal of Electrical Power and Energy Systems*, 157, 2024.

[20] Junxian Li, Weihao Hu, Xiawei Wu, Qi Huang, Zhou Liu, Zhe Chen, and Frede Blaabjerg. A hybrid cable connection structure for wind farms with reliability consideration. *IEEE Access*, 7:144398–144407, 2019.

[21] Chunhua Li, Han Diao, Yijing Chen, Yabo Zhu, Shaowei Huang, Xiaowei Zeng, and Zerong Zeng. Simulation and calculation of maximum transmission power for offshore wind plants accounting for the electro-magnetic transient process. *Energy Reports*, 9:32–37, 2023. The 8th International Conference on Sustainable and Renewable Energy Engineering.

[22] Franco P. Preparata and Michael Ian Shamos. Intersections. In *Computational Geometry*, pages 266–322, New York, NY, 1985. Springer New York.

[23] Anna Beer, Dominik Seeholzer, Nadine Sarah Schüler, and Thomas Seidl. Angle-based clustering. In *Similarity Search and Applications*, pages 312–320, Cham, 2020. Springer International Publishing.

[24] Shankha Shubhra Goswami. Outranking methods: Promethee i and promethee ii. *Foundations of Management*, 12(1):93–110, 2020.